ALTERATIONS IN RETROGRADE AXONAL TRANSPORT IN OPTIC NERVE OF TYPE I AND TYPE II DIABETIC RATS

Zhang, Lixin

Ino-ue, Masao

Dong, Kai

Yamamoto, Misao

(Citation)
The Kobe journal of the medical sciences,44(5):205-215

(Issue Date)
1998-12

(Resource Type)
departmental bulletin paper

(Version)
Version of Record

(URL)
https://hdl.handle.net/20.500.14094/E0001013

Kobe J. Med. Sci. 44, 205/215, December 1998

ALTERATIONS IN RETROGRADE AXONAL TRANSPORT IN OPTIC NERVE OF TYPE I AND TYPE II DIABETIC RATS

Lixin ZHANG*, Masanori INO-UE*, Kai DONG †,
and Misao YAMAMOTO*

*Department of Ophthalmology, Kobe University School of Medicine
† First Department of Anatomy, Kobe University School of Medicine

INDEXING WORDS

diabetes mellitus; Fluoro-Gold labeling; retinal ganglion cell; retrograde axonal transport

SYNOPSIS

Clinical and electrophysiological examinations have yielded visual pathway function abnormalities in both humans and animal models with diabetes mellitus (DM). However, subclinical involvement of the optic nerve has not yet been fully investigated. In this study, we demonstrated the different impairments in retrograde axonal transport occurring in selective retinal ganglion cells (RGCs) of Type I and II diabetic rats. Rats were injected with streptozotocin (STZ) to induce Type I DM. The Otsuka Long-Evans Tokushima Fatty (OLETF) rats represented the Type II DM group. The STZ-induced (Type I) diabetic rats had low body weights and significant elevations in blood glucose levels compared with the age-matched control rats. On the contrary, the OLETF rats (Type II) had high body weights and significant elevations in blood glucose concentrations compared with the age-matched controls. Fluoro-Gold (FG) was injected into the bilateral dorsal lateral geniculate nucleus. Accumulation of FG in large and medium type RGCs in STZ-induced diabetic rats was significantly decreased compared with the controls. However, the accumulation of FG in RGCs of OLETF rats did not show a significant decrease compared with the controls. Our findings suggest that, within the time frame of study, retrograde axonal transport impairment of large and medium type RGCs

Received for publication : October 30, 1998
Authors' names in Japanese : 張　力新、井上正則、董　　凱
山本　節

in the STZ-induced (Type I DM) diabetic rats was greater than in the OLETF (Type II DM) diabetic rats. Impairment of retrograde axonal transport in Type I diabetes may precede or be a consequence of metabolic dysfunctions in the large and medium-sized RGCs eventually leading to optic nerve atrophy.

INTRODUCTION

Diabetic neuropathy is characterized by signs and symptoms of peripheral sensory, motor and autonomic nerve dysfunction. [3] Histopathological, biochemical and electrophysiological changes have been demonstrated in the peripheral nerves of experimental diabetic animals. [7,10,17,22] Metabolic factors related to hyperglycemia and several other unknown variables have been implicated in peripheral neuropathies in diabetic subjects. These peripheral neuropathies have been reported to differ between Type I and II diabetes mellitus (DM) in both rat and human subjects. [18] In Type I DM, widespread axonal degeneration with axonal transport impairment and myelin wrinkling occurs in the nerve fibers. This is in contrast to Type II DM where the mild elevation in blood glucose concentrations leads to a more localized fiber damage characterized by Wallerian degeneration and ischemia which is unrelated to aging.

In the nerve cell, proteins associated with axonal structure and synaptic transmitter function are synthesized in the cell body and subsequently carried by the anterograde transport system to the axon and its terminals. In the opposite direction, the retrograde transport of macromolecules is suggested to act as a messenger system safeguarding the integrity of the entire neuron. [11] Axonal transport, therefore, plays a basic role in maintaining the structural integrity of the axon, and its impairment may be the primary event in several neuropathies, including those characterized by axonal degeneration. We therefore investigated the impairment of selective retinal ganglion cells (RGCs) in streptozotocin (STZ)-diabetic rats and the Otsuka Long-Evans Tokushima Fatty (OLETF) rats using a fluorescent retrograde labeling technique.

MATERIALS AND METHODS

Animals and Induction of Diabetes

Male Wistar albino rats (6 weeks old, weighing about 200 g, Japan Clea Co., Japan), OLETF and Long-Evans Tokushima Otsuka (LETO) rats were used in this study. The animals were treated under the Guidelines for Animal Research of Kobe University and in accordance with the Declaration of Helsinski and the Guiding Principles in the Care and Use of Animals.

Type I DM was induced in the Wistar albino rats by an intraperitoneal injection of STZ (Sigma, St. Louis, MO) in 0.01 M citrate (pH 4.5) at a dosage of 70 mg/kg body wt. Age- and weight-matched control rats received an intraperitoneal injection of citrated buffer in identical amounts and pH. The OLETF rats served as the Type II DM group with the LETO rats as the corresponding control group. In the STZ-induced diabetic rats, fasting blood glucose levels were measured 48 hrs after intraperitoneal injection, then every two weeks and before sacrifice. The fasting blood glucose levels in the OLETF and LETO rats were measured every two weeks throughout the experiment and before sacrifice. The STZ-induced diabetic rats were weighed before the injection and at two week intervals. All the other groups were also weighed at 2 week intervals throughout the experiment.

Retrograde fluorescent labeling of RGCs

Retrograde fluorescent labeling of RGCs was done as follows. Briefly, the rats were anesthesized with an intraperitoneal injection of 5% pentobarbital sodium (0.5 ml/kg wt) and then positioned in a stereotaxic frame (Narishige, SR-6). Two small holes were drilled into the skull at the site corresponding to the bilateral dorsal lateral geniculate nucleus (dLGN). Glass micropipettes with internal diameters of 20 μm were loaded with 4% Fluoro-Gold (FG, Fluorochrome Inc.) dissolved in distilled water, then stereotaxically lowered into the bilateral dLGN. The dye was injected iontophoretically, applied intermittently (7-sec on/off cycles) at 3 μA charge for 10 min. The micropipette was left in place for an additional 10 min. to allow for complete diffusion of the dye into the tissues. Postoperatively, all of the animals were left in a dark room. After 72 hours, the rats were put under deep anesthesia, then perfused with 200 ml of saline followed by 1000 ml of 4% formaldehyde in 0.1M neutral phosphate buffer (pH 7.3). Prior to enucleation, the center of insertion of the superior rectus muscle was marked with 0.1% cresyl violet. The brain and one eyeball of each rat were excised and the retina was freed from the pigment epithelium and mounted vitreal side up on a non-fluorescent gelatin-coated glass slide by making incisions that extend radially from the dorsal, ventral, nasal and temporal poles to the optic disc. The dorsal pole corresponded to the median line of the previously marked insertion of the superior rectus muscle. After air-drying in a dark box, the retinal specimen was viewed by a fluorescence microscope (Nikon Optiphoto-EF, Japan). A UV filter system (main excitation wavelength 360nm) was used to identify the cells labeled with FG. The retina was first divided into 72 areas. The distribution of labeled cells was plotted on an outline drawing of these 72 microscopic fields then photographed individually. The brain was sectioned serially on a cryostat in the coronal plane at a thickness of 40 μm. Every fifth section was mounted on a

gelatin- coated glass slide. The exact site of injection, as well as the extent of diffusion within each structure, was confirmed under the fluorescence microscope. Results were considered only if the injection had labeled the dLGN adequately without involvement of neighboring nuclei. Seven control and seven STZ-induced diabetic rats, six OLETF and five LETO rats were considered for analysis.

Estimation of Fluoro-Gold labeled RGCs

The photographs of the retina were processed by a microcomputer imaging device (NIH, Image 1.44). RGC soma sizes were measured manually by encircling each cell in each microscopic field and were classified into three types, Type 1: more than 20 μ m, Type 2: 16~ 20 μ m and Type 3: less than 15 μ m respectively. [16] Next, the labeled cells in each microscopic field were counted manually and the percentages of the population of each type of RGCs in the control and diabetic retina (Type I and II DM) groups were estimated.

Nissl staining

After viewing under the fluorescence microscope, the wholemount retinal specimens were stained with 0.1% cresyl violet and photographed in the plane of the ganglion cell layer as described previously[19]. The percentage of the population of each RGC type in the retina was calculated using the same method as above.

For statistical analysis, data from experimental and control groups were compared using the Student's t -test. A probability level of 5% was set for statistical significance.

RESULTS

Diabetes

The STZ-induced diabetic rats showed a significant high level of blood glucose concentration and low body weight throughout the experimental period (Table I). The blood glucose concentration of OLETF rats began to increase 20 weeks after birth, and then increased gradually accompanied with a increase of body weight. At the end of the experiment, the blood glucose and body weight of OLETF rats were significant higher than those of the contol rats (Table II).

TableI. Body weight and blood glucose of the STZ-diabetic rats before sacrifice.

	Body weight (g)	Blood glucose (mg/dl)
Control (n=7)	516.6 ± 41.0	106.1 ± 9.3
Diabetes (n=7)	285.2 ± 34.4	627.9 ± 63.6

TableII. Body weight and blood glucose of the OLETF and LETO rats.

	6 weeks after birth		Before sacrifice	
	LETO (n=5)	OLETF (n=6)	LETO (n=5)	OLETF (n=6)
Body weight (g)	216.0 ± 11.5	273.2 ± 13.1	536.0 ± 24.5	625.3 ± 64.1
Blood glucose (mg/kg)	84.2 ± 5.0	99.7 ± 7.3	98.8 ± 3.6	468.3 ± 41.2

Retrograde axonal transport

The bilateral dLGN injection sites demonstrating the main features of dLGN afferents and their topographic organization are illustrated in Fig.1. All cases having the same features as above were included in the analysis. FG-labeled RGCs were identified as large, medium and small cells (Figs.2A & 3A). After manually counting all FG-labeled RGCs in each microscopic field, the percentage of each RGC type was computed.

A) STZ-diabetic rats

The average numbers of FG labeled large, medium and small RGCs in the normal retina were 31.14±11.63, 273.29±95.51 and 3073.71±1418.97, respectively, as shown in Table 3. The average proportion of each type of RGCs were calculated to be 0.95±0.15% (large), 8.43±1.13% (medium) and 90.62±1.24% (small). In STZ-induced diabetic retina, the large type of RGCs were rarely found (Fig.2B). The average number of FG-labeled large and medium RGCs in diabetic retina were 6.86±5.11 and 213.57±88.10 respectively, as shown in TableⅢ. These values were less than those in the control retina. The mean percentage of large type RGC in diabetes was 0.22±0.16% which corresponds to a significant decrease compared to age- matched controls (p <0.0001). The mean percentage of medium type RGC was also significantly different in diabetes and controls, measuring 6.56±1.40% in diabetes and 8.43±1.13% in controls (p <0.05).

B) OLETF diabetic rats

The average numbers of FG labeled large, medium and small RGCs in the retina of normal LETO rats were 23.80±4.60, 257.20±61.23 and 2569.60±460.94 respectively, as shown in TableⅣ. In the OLETF diabetic retina, the sizes of the FG-labeled RGCs did not differ from the normal control LETO rats (Fig. 3B). The average number of FG-labeled large, medium and small RGCs in diabetic retina were 20.33±4.32, 242.83±49.20 and 2694.67±508.27 respectively, as shown in Table 4. Statistical analysis showed no significant difference in the population of each type of RGC in the retinas of the OLETF diabetic and control LETO rats (Large cell: p >0.05; Medium cell: p>0.05; Small cell: p >0.05).

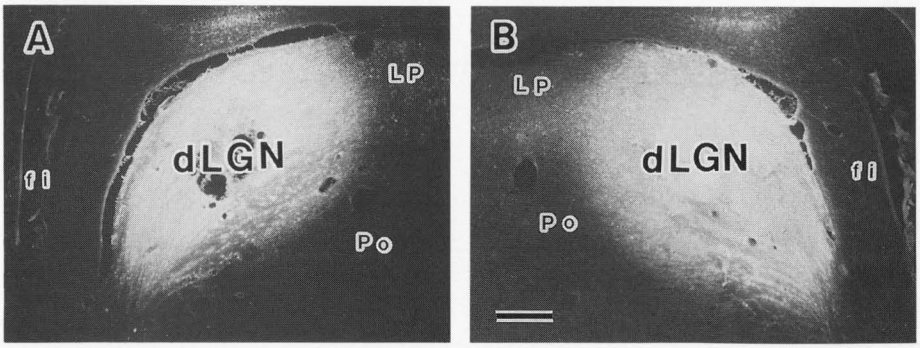

Fig. 1. Injection sites of Fluoro-Gold in the bilateral dorsal lateralgeniculate nucleus. dLGN; dorsal lateral geniculate nucleus. fi; fimbria hippocampus. LP; lateral posterior thalamus nuclei. Po; posterior thalamus nuclei group.
A. Right side. B. Left side. Scale bar=0.6mm

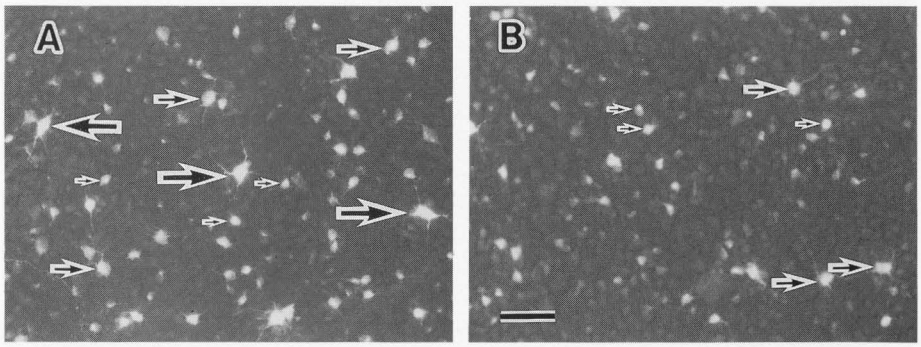

Fig. 2. Retrogradely-labeled retinal ganglion cells. Large, medium and small arrows show large type, medium type and small type retianl ganglion cells, respectively.
A. Controls. B. Streptozotocin-diabetic rats. Scale bar=60 μ m

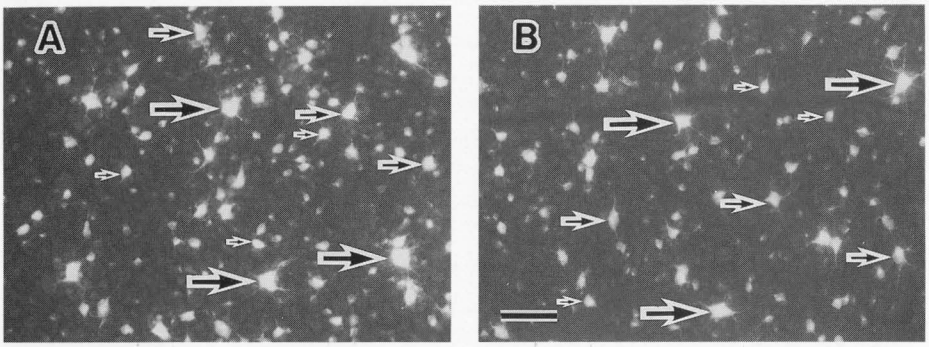

Fig. 3. Retrogradely-labeled retinal ganglion cells. Large, medium and small arrows show large type, medium type and small type retianl ganglion cells, respectively.
A. Controls. B. Otsuka Long-Evans Tokushima Fatty diabetic rats. Scale bar=60 μ m

Histological study by Nissl method

After observation under fluorescence microscope, the retinas were stained by the Nissl method. Light microscopic examination revealed the somata of large, medium and small-type RGCs in both normal and STZ-diabetic retinas (Figs.4A & 4B). Although the perikaryon of the RGCs in diabetic retinas showed slight shrinkage, this was not statistically significant. Furthermore, neither significant degeneration nor cell loss was observed. Statistical analysis showed no significant difference in the population of each type of RGC in the retinas of the diabetic and control rats (Large : p >0.05; Medium : p >0.05; Small : p >0.05).

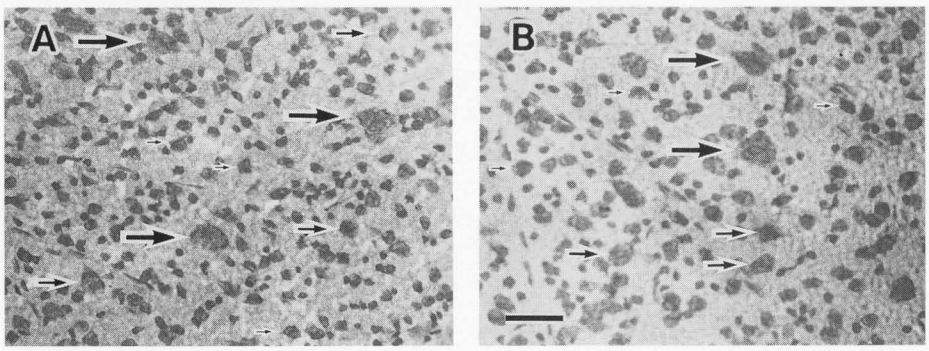

Fig. 4. Retinal ganglion cell layers of a wholemount retina stained by Nissl method. Large, medium and small arrows show large type, medium type and small type retianl ganglion cells, respectively.
A. Controls B. Streptozotocin -diabetic rats. Scale bar=30 μ m

Table Ⅲ. The average number and percentage of each type of FG labeled RGCs in the STZ-diabetic rats.

	Large cell Number (%)	Medium cell Number (%)	Small cell Number (%)
Control (n=7)	31.14 ± 11.63 (0.95 ± 0.15)	273.29 ± 95.51 (8.43 ± 1.13)	3073.71 ± 1418.97 (90.62 ± 1.24)
Diabetes (n=7)	6.86 ± 5.11 (0.22 ± 0.16)	213.57 ± 88.10 (6.56 ± 1.40)	3119.86 ± 1286.29 (93.22 ± 1.51)

Table Ⅳ. The average number and percentage of each type of FG labeled RGCs in the OLETF rats.

	Large cell Number (%)	Medium cell Number (%)	Small cell Number (%)
LETO (n=7)	23.80 ± 4.60 (0.84 ± 0.07)	257.20 ± 61.23 (9.05 ± 1.23)	2569.60 ± 508.27 (90.02 ± 1.15)
OLETF (n=7)	20.33 ± 4.32 (0.74 ± 0.14)	242.83 ± 49.20 (8.27 ± 0.74)	2694.67 ± 508.27 (91.25 ± 0.72)

DISCUSSION

Animal models of DM can be classified into two groups as chemically induced hyperinsulinemic models of Type I DM and the genetically induced models of Type I and Type II DM. Although several studies on the pathogenesis of neuropathy have been conducted with animal models of Type I DM, [8,9,12,13,14] studies on Type II DM models are still rare. [15] To that end, we used STZ-induced Type I diabetic rats and OLETF (Type II) diabetic rats to study the neuropathological features in optic nerves of both models. Several morphometric studies on peripheral nerves of Type I diabetic rats revealed reduction of axon size and cross-sectional area, loss of axonal neurofilaments and atrophy of nerve fibers. [12-14] It is already known that retinal protein biosynthesis is significantly reduced and slow anterograde axonal transport is secondarily impaired. [1,2] Functional data provided evidence about accumulation of retrogradely transported glycoproteins in the sciatic nerve of Type I diabetic rats and reduction in retrograde axonal transport of nerve growth factor (NGF), transmitter enzymes and fucose-labeled protein, which all may induce misinformation for structural protein synthesis in the nerve cell body. [4,20] In this study, we found that FG labeling of large and medium sized RGCs decreased significantly in type I diabetic rats whereas Nissl staining showed no evidence of reduction in RGC population. Previous studies have shown a decrease in the cross-sectional

area of the distal segment of peripheral axons[8,21,22] and reduction in optic nerve myelinated fiber caliber of diabetic rats, particularly in the large fibers.[5,6] This leads us to suggest that decreased retrograde axonal transport in larger ganglion cells precede the morphological impairment of the larger myelinated fibers of optic nerve. Furthermore, no significant decrease of FG-labeling of the large and medium sized RGCs was observed in OLETF rats. These results suggest that there is a selective impairment in retrograde axonal transport of large and medium sized RGCs in type I diabetic rats without shrinkage of the perikaryon or loss in ganglion cell population.

On the other hand, retrograde axonal transport was not impaired during the experimental period in OLETF diabetic rats. The characteristic features of OLETF rats include the late onset of DM, chronicity, mild form of obesity and renal complications; all closely resembling those of human Type II DM. Although OLETF rats in this report did not demonstrate any significant pathological abnormalities in the optic nerve, a longer study might have revealed changes in the diabetic optic nerve. Recent reports suggest that sucrose-fed OLETF rats develop numerous pathophysiological abnormalities in the peripheral nerve.[20] These observations point out to the importance of hyperglycemia and increased polyol pathway activity in the development of diabetic neuropathy. We believe that further work on hyperglycemic OLETF rats is highly essential to highlight the pathogenetic mechanisms of diabetic neuropathy in Type II DM which is the major type of human diabetes.

ACKOWLEDGMENTS

This paper was presented at the 64th Annual Meeting of the Mid-Japan Ophthalmological Society at Yokkaichi City, Mie Prefecture, October 2nd-5th, 1998. The authors also wish to express their thanks to Mr.Tomiyoshi Setsu of the Kobe University Department of Anatomy for his expert technical assistance.

REFERENCES

1. Chihara, E.: J. Neurochem. 1981.37. 247/250. Impairment of protein synthesis in the retinal tissue in diabetic rabbits: Secondary reduction of fast axonal transport.
2. Chihara, E., Sakugawa, M., and Entani, S.: Brain Res. 1982. 250. 363/366. Reduced protein synthesis in diabetic retina and secondary reduction of slow axonal transport.
3. Harati, Y.: Ann. Intern. Med. 1987.107. 546/559. Diabetic peripheral neuropathies.
4. Hellweg, R. and Hartung, H.D.: J. Neurosci. 1990. Res. 26. 258/267. Endogenous levels of nerve growth factor (NGF) are altered in experimental diabetes mellitus: a possible role for NGF in the pathogenesis of diabetic neuropathy.

5. Ino-ue, M., Yokogawa, H., Yamamoto, M., Naka, H., and Kuriyama, H.: Exp. Eye Res. 1998. 66. 397/401. Structural impairments in optic nerve of diabetic rats ameliorated with the aldose reductase inhibitor.
6. Ino-ue, M., Ohgiya, N., and Yamamoto, M.: Brain Res. 1998. 800. 319/322. Effect of aminoguanidine on optic nerve involvement in experimental diabetic rats.
7. Jefferys, J.G., Palmano, K.P., Sharma, A.K., and Thomas, P.K.: J. Neurol. Neurosurg. Psychiatry. 1978. 41. 333/339. Influence of dietary myoinositol on nerve conduction and inositol phospholipids in normal and diabetic rats.
8. Jakobson, J.: Diabetologia. 1976. 12. 539/546. Axonal dwindling in early experimental diabetes. I. A study of cross sectioned nerves.
9. Jakobsen, J., Brimijion, S., Skau, K., Sidenius, P., and Wells, D.: Diabetes. 1981. 30. 797/803. Retrograde axonal transport of transmitter, enzymes, fucose-labeled protein, and nerve growth factor in streptozotocin-diabetic rats.
10. Kador, P.F.: Med. Res. Rev. 1988. 8. 325/352. The role of aldose reductase in the development of diabetic complications.
11. Kristensson, K. and Olsson, Y.: Prog. Neurobiol. 1973. 1. 87/109. Diffusion pathways and retrograde axonal transport of protein tracers in peripheral nerves.
12. Medori, R., Gambetti, L.A., Monaco, S., and Gambetti, P.: Pro. Natl. Acad. Sci. USA. 1985. 82. 7716/7720. Experimental diabetic neuropathy: Impairment of slow transport with changes in axon cross-sectional area.
13. Medori, R., Gambetti, L.A., Jenich, H., and Gambetti, P.: Neurology. 1988. 38. 597/601. Changes in axon size and slow axonal transport are related in experimental diabetic neuropathy.
14. Medori, R., Jenich, H., Gambetti, L.A., and Gambetti, P.: J. Neurosci. 1988. 8. 1814/1821. Experimental diabetic neuropathy: similar changes of slow axonal transport and axonal size in different animal models.
15. Nakamura J., Koh, N., Sakakibara, F., Hamada, Y., Wakao, T., Sasaki, H., Mori, K., Nakashima, E., Naruse, K., and Hotta, N.: Life Sci. 1997. 60. 1847/1857. Diabetic neuropathy in sucrose-fed Otsuka Long-Evans Tokushima fatty rats: effect of an aldose reductase inhibitor.
16. Perry, V.H.: Proc. R. Soc. Lond. B. Biol. Sci. 1979. 204. 363/375.The ganglion layer of retina of the rat: a Golgi study.
17. Sharma, A.K. and Thomas, P.K.: J. Neurol. Sci.1974. 23. 1/15. Peripheral nerve structure and function in experimental diabetes.
18. Sima, A.A.F., Nathaniel, V., Bril, V., McEwen, T.A.J., and Green, D.A.:J. Clin. Invest. 1988. 81. 349/364. Histopathological heterogeneity of neuropathy in insulin-dependent

and non-insulin-dependent diabetes, and demonstration of axo-glial dysjunction in human diabetic neuropathy.

19. Schober, W. and Gruschka, H.: Z. mikrosk-Anat. Forsch. 1977. 91. 397/414. Die gonglion zelle der retina der albinoratte: eine qualitative und quantitative studie.
20. Sidenius, P. and Jakobsen, J.: Diabetologia. 1981. 20. 110/112. Retrograde axonal transport: a possible role in the development of neuropathy.
21. Sharma, A.K. , Bajada, S., and Thomas, P.K.: Acta Neuropathol. 1981. 53. 257/265. Influence of streptozotocin-induced diabetes on myelinated nerve fiber maturation and on body growth in the rat.
22. Yagihashi, S., Kamijo, M., and Watanabe, K.: Am. J. Pathol. 1990. 136. 1365/1373. Reduced myelinated fiber size correlates with loss of axonal neurofilaments in peripheral nerve of chronically streptozotocin diabetic rats.